Journal of Environmental Management 270 (2020) 110823

Contents lists available at ScienceDirect

Journal of Environmental Management

journal homepage: http://www.elsevier.com/locate/jenvman

Research article

Increasing phosphate sorption on barium slag by adding phosphogypsum for non-hazardous treatment

Tengfei Guo [a,b], Hannian Gu [a,b,*], Shicheng Ma [c], Ning Wang [a]

[a] Key Laboratory of High-temperature and High-pressure Study of the Earth's Interior, Institute of Geochemistry, Chinese Academy of Sciences, Guiyang, 550081, China
[b] University of Chinese Academy of Sciences, Beijing, 100049, China
[c] School of Geography and Environmental Science, Guizhou Normal University, Guiyang, 550025, China

ARTICLE INFO

Keywords:
Barium slag
Phosphate
Adsorption capacity
Models
Sorption mechanisms

ABSTRACT

Barium slag (BS) is a waste residue in the barium salt industrial procedure. Due to its high leaching concentration of Ba^{2+}, BS is classified as a kind of hazardous waste. Industrial waste phosphogypsum (PG) is effective to immobilize barium ion in BS owing to the slightly soluble sulfate included. In this study, two different proportions of PG were selected for mixing with BS to solidify soluble barium ion. The non-hazardous BS samples treated with the proportions of PG (BS-PG1, BS-PG3) were then functionally used for phosphate removal in solution. Batch experiments for removal of phosphate were performed to evaluate the adsorption efficiency of BS-PG1 and BS-PG3. The effect of various factors such as contact time, initial pH, and reaction temperature on sorption performance was investigated. BS-PG1 and BS-PG3 reached adsorption equilibrium in approximately 3h at the initial concentration of 15 mg/L, and BS-PG1 exhibited adsorption capacity of 12.47 mg P/g, higher than that of BS (11.49 mg P/g) under the condition of solid:liquid, 1g:1L, 25 °C, natural pH. The results show that the adsorption processes of phosphates ions onto both BS-PG1 and BS-PG3 fitted well with the pseudo-second-order kinetic model. The Langmuir isothermal model was considered as the appropriate equation for experimental data, showing a maximum adsorption capacity for phosphate up to 13.67 mg P/g and 11.59 mg P/g for BS-PG1 and BS-PG3. In comparison with other adsorbents, BS-PG1 and BS-PG3 could be considered as efficient materials for the removal of phosphate.

1. Introduction

Barium slag (BS) is a kind of solid waste generated during the treatment of barite using the process of carbothermal reduction. In the production process of barium salt, barite is reduced to barium sulfide by coke or coal in a rotary kiln at about 1100 °C (Jamshidi and Ebrahim, 2008; Salem and Osgouei, 2009). After leaching with hot water, the product obtained from the carbothermic process consists of barium sulfide solution and impurities (Salem and Jamshidi, 2012; Guzmán et al., 2012). Barium slag is then discharged after filtration of barium sulfide solution (Gu et al., 2019). It is estimated that the production of 1 ton of barium salt generates approximately 0.8–1 ton of barium slag. The annual production capacity and output of China's barium carbonate accounts for more than 70% in the world (Wang et al., 2016). Therefore, barium slag is basically generated in China, and it poses considerable negative environmental threats. Currently, a large amount of discharged barium slag is mainly disposed of through landfills (Vaidya et al., 2010), occupying the land and bringing many hazards.

Barium slag contains a large amount of water-soluble barium and acid-soluble barium. The leaching concentration of Ba^{2+} is usually more than 1000 mg/L (Gu et al., 2019). The water-soluble barium and acid-soluble barium in the BS can be infiltrated into the soil after being washed by rain, causing serious damages to the soil and groundwater (Menzie et al., 2008). In addition, the water-soluble barium ion is highly toxic, posing a potential toxicity risk to plants and animals (Lamb et al., 2013). According to the *Identification standards for hazardous wastes*, barium ion concentrations of the solution should not exceed 100 mg/L (SEPA and AQSIQ, 2007). As the result of high barium ion dissolution concentrations, BS is classified as a kind of hazardous solid wastes. Due to the enormous quantities and toxic properties, the management, disposal and utilization of BS has become a significant issue for barium salt production enterprises.

* Corresponding author. Key Laboratory of High-temperature and High-pressure Study of the Earth's Interior, Institute of Geochemistry, Chinese Academy of Sciences, Guiyang, 550081, China.
E-mail address: guhannian@vip.gyig.ac.cn (H. Gu).

https://doi.org/10.1016/j.jenvman.2020.110823
Received 5 February 2020; Received in revised form 27 April 2020; Accepted 21 May 2020
Available online 15 June 2020

It has been reported that the remaining barium in BS can be recovered to produce barium chloride and barium nitrate (Dong et al., 2003). BS can also be used as an additive in cement (Jiang, 2007) or for producing building bricks (Liu et al., 2017). In addition, investigations have been extended to develop BS as an adsorbent to remove harmful and toxic materials from water, such as PO_4^{3-} (Yao and Zhao, 2010), Cr^{6+} (Ding, 2005), and SO_4^{2-} (Mulopo and Motaung, 2014). However, most of the above cases use original BS without non-hazardous treatment. Recently, China implements more stringent control on hazardous wastes, and BS cannot be used directly without harmless treatment.

Many attempts have been made to solidify soluble barium ion in BS, and sulfate-containing additives, such as sodium sulfate (Yuan et al., 2016), ferrous sulfate, manganese residue (Liu et al., 2016) and phosphogypsum (PG) (Gu et al., 2019), are proposed for industrial application or laboratory scale research. PG is one of the by-products of wet process phosphoric acid production, and it consists primarily of calcium sulfate dihydrate ($CaSO_4{\cdot}2H_2O$) and trace impurities (Rashad, 2017). With the mass ratios of 10:1–20 (BS:PG), the mixtures were demonstrated to be harmless. However, to explore new paths for application of non-hazardous BS treated with PG appears to be also important. The propose of the current study is to know the adsorption performance of BS on phosphate solution after treatment with PG. According to the previous results (Gu et al., 2019), two different ratios of BS:PG, 10:1 and 10:3, were selected in this study to investigate their adsorption behavior. The adsorption characteristics of these materials for phosphate removal from aqueous solutions were evaluated in batch adsorption experiments. The influences of some operation parameters on phosphate removal were investigated, including contact time, initial pH, reaction temperature. Pseudo-first-order and pseudo-second-order models and isotherm models of Langmuir and Freundlich were applied to describe the adsorption process.

2. Materials and methods

2.1. Preparation of materials

The BS used in this study was obtained from a barium chemical enterprise located in Yuping, Guizhou, China. PG sample was supplied by Kailin Group, Guizhou, which is a phosphate chemical enterprise. The main compositions of BS are BaO 40.5%, SO_3 21.6%, SiO_2 15.55%, CaO 9.57%, Fe_2O_3 4.64%, P_2O_5 2.05%, etc., while PG used in this study are CaO 35.9%, SO_3 53%, SiO_2 5.12%, P_2O_5 2.05%, and some other impurities as previously reported (Gu et al., 2019). Both the samples were dried at 105 °C until constant weights. Subsequently, samples were pulverized using a motar and pestle and sieved to < 75 μm in size. Then, BS-PG1 and BS-PG3 were prepared as adsorbents by mixing BS with PG at a ratio of 10:1 and 10:3, respectively.

2.2. Analysis and characterization

The chemical composition of BS, BS-PG1 and BS-PG3 were characterized by X-ray diffractometer (XRD, PANalytical Empyrean, Netherlands). The functional groups of three materials were performed by infrared analysis (FTIR, VERTEX 70, Brock, Germany). Inductively coupled plasma atomic emission spectrometer (ICP-AES, Agilent 5100) was used to analyze the metal ion concentrations in solutions after adsorption (0, 10, and 15 mg P/L). The concentration of phosphorus in the solution filtered from phosphorus releasing test, batch phosphate adsorption experiments and desorption experiments was measured by the molybdate blue spectrophotometric method using UV9100C spectrophotometer at λ of 700 nm (Lin et al., 2018).

2.3. Phosphorus releasing test

PG was reported containing soluble phosphorus (Li et al., 2017) and in this study releasing phosphorus of original materials (BS and PG) and the adsorbents (BS-PG1 and BS-PG3) were investigated before adsorption experiments. Specifically, 0.25 g of original material/adsorbent was added to 250 mL prepared solution, and the initial pH of the solution was adjusted with diluted HCl or NaOH solution (Papaslioti et al., 2018). After reacting for 10 h with a shaking rate of 200 rpm, the final pH was determined and the supernatants were filtered using a 0.45 μm membrane filter for phosphate determination.

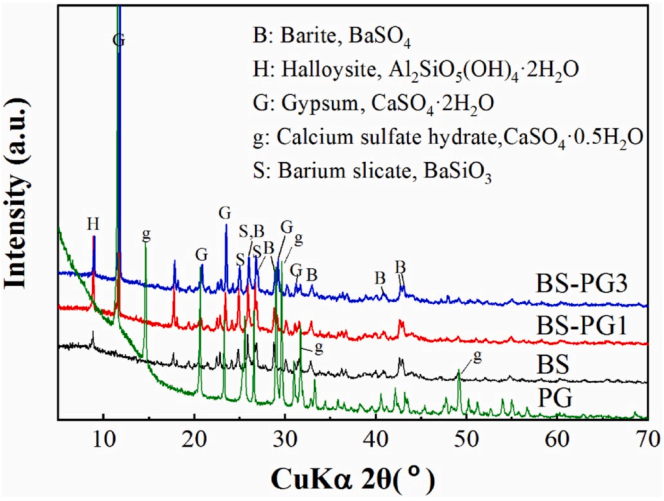

Fig. 1. X-ray diffractogram of BS, PG, BS-PG1, and BS-PG3.

2.4. Batch adsorption experiments

Phosphate stock solution was prepared by dissolving potassium dihydrogen phosphate (Guaranteed Reagent, Tianjin Kemiou Chemical Reagent Co., Ltd, China). All solutions used in this experiment were prepared by deionized water. The adsorption reactions were conducted in a series of 250 mL glass conical flasks and the flasks were placed in a Water-bathing Constant Temperature Vibrator for a particular period of time and with a shaking rate of 200 rpm. To investigate adsorption kinetic behavior, preselected concentrations of phosphate (5, 8, 10, and 15 mg P/L) and 0.25 g of adsorbent per 250 mL of solution were used. In the experiments, the temperature was kept constant at 25 °C except for the experiments in which the effect of reaction temperatures were investigated. Supernatants were collected at various time intervals by filtering using 0.45 μm membranes. For pH optimization, the initial pH values of the solutions were adjusted to the range of 1.0–13.0 through HCl or NaOH. Reaction temperatures of 25, 30, 35, 40, and 50 °C were set to observe the effect of temperature on adsorption. The isothermal adsorption tests were carried out by adding 0.25 g of sample in a 250 mL of 5–30 mg P/L.

In addition, phosphate desorption experiments were performed with BS, BS-PG1, BS-PG3. All the materials were previously used to adsorbed 15 mg P/L phosphate solution. In this section, deionized water was used to conduct desorption experiments on samples (0.1g:100 mL), the other experimental conditions were controlled at 25 °C, natural pH and the reactions lasted for 10 h.

In this paper, all experiments were carried out triplicate in order to effectively reduce the experimental error.

The phosphate adsorbed per unite weight of adsorbent was evaluated by Eq. (1)

$$q_e = (C_i - C_f)V / m \quad (1)$$

where q_e (mg/g) indicates the equilibrium amount of phosphate adsorbed per unit mass of adsorbents, C_i and C_f are the initial and the equilibrium concentrations of phosphate in solution (mg/L), respectively, V is the solution volume (L), and m represents the weight of sorbent (g).

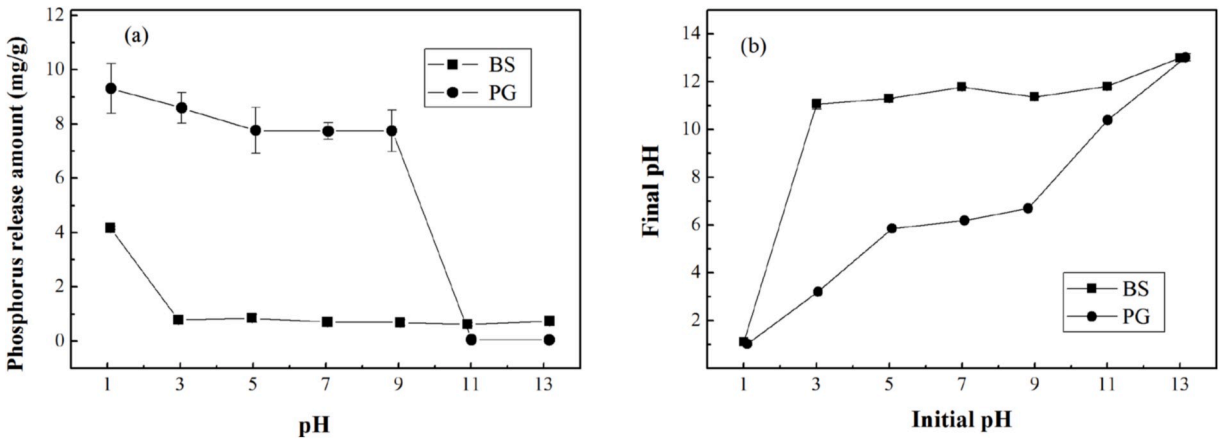

Fig. 2. (a) Phosphorus release from BS and PG at different initial pH and, (b) the final pH of BS and PG.

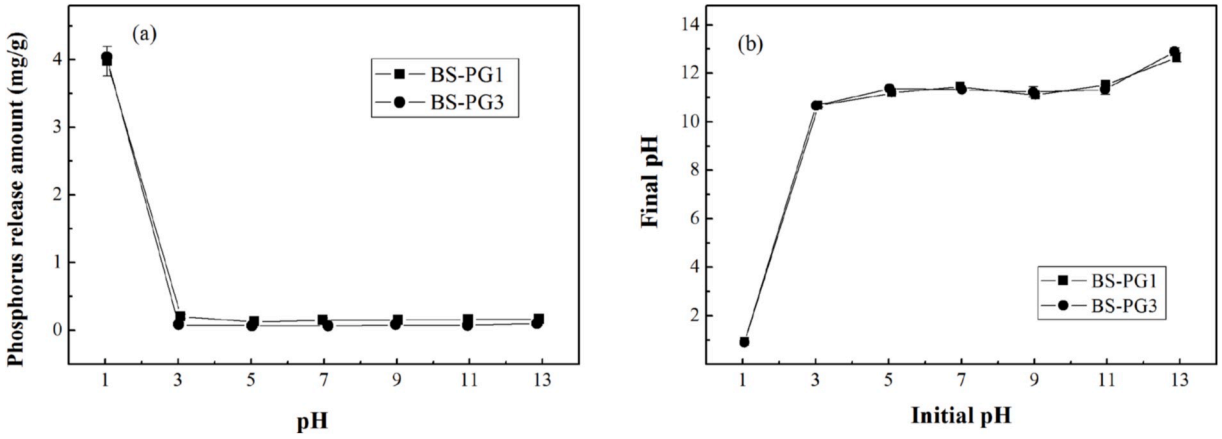

Fig. 3. (a) Phosphorus release from BS-PG1 and BS-PG3 at different initial pH, and (b) the final pH of BS-PG1 and BS-PG3.

3. Results and discussion

3.1. Sample characterization

The XRD patterns of BS, PG, and the mixtures with PG are presented in Fig. 1. It can be observed that major crystalline phases of BS are barite, halloysite and barium silicate, and PG contains calcium sulfate dihydrate and calcium sulfate hemihydrate as some literatures reported (Rashad, 2017; Jiang et al., 2019). Barium sulfide was identified as the source of soluble barium in the BS (Liu et al., 2017), which is not presented in the XRD pattern due to the low limit of detection. As PG added, the XRD patterns show a remarkable difference compared to the untreated BS material. The characteristic peaks of calcium sulfate dihydrate appears after PG added, and with the proportion of PG increasing, the strength of peaks increases. Meanwhile, calcium sulfate hemihydrate disappears while PG is in contact with BS for the alkaline can promote the formation of calcium sulfate dihydrate (Li et al., 2013).

PG has been used as a modifier for application of remediation, alkaline stabilization or adsorption capacity improvement (Lopes et al., 2013; Cuadri et al., 2014; Xue et al., 2019). In this study, On the basis of using the soluble sulfate ions from PG to stabilize barium ion in BS (Gu et al., 2019), the BS adding PG is also expected to enhance the phosphate adsorption capacity.

3.2. Phosphorus releasing test

Before the materials were taken to adsorb phosphorus, the phosphorus release should be investigated to obtain more reliable results. Figs. 2 and 3 show the release of phosphate at different pH conditions and the changes of pH before and after the reaction for 10 h. It can be seen from Fig. 2a that low pH conditions are more conducive to the release of soluble phosphate in the samples. In terms of PG, the release of phosphorus is greater than 7 mg/g at pH < 9, and the release of phosphorus is significantly reduced under alkaline conditions. It has been reported that PG can release phosphate in aqueous solution (Li et al., 2017). This could be assigned to the fact that a strong acidic solution can dissolve calcium phosphate (Sakai et al., 2016), while an alkaline environment tends to produce phosphate precipitates from different chemical forms (Liu et al., 2015). The final pH of the PG releasing system presents a slow increase at the initial pH of 5.0–9.0 and it could be due to the sulfate content in PG (Fig. 2b).

In BS samples, the release of phosphorus is less than 1.0 mg/g under most of the pH conditions. However, under extremely acidic condition (pH = 1), the amount of phosphorus released from BS is as high as 4.17 mg/g. The BS is alkaline leading to the final pH values (exception of initial pH at 1.0) to be alkaline as shown in Fig. 2b. As discussed, the alkaline condition produce precipitate of calcium phosphate, and the releasing phosphorus is no more than 0.85 mg/g at the initial pH from 3.0 to 13.0. BS-PG1 and BS-PG3 display a similar tendency with BS (Fig. 3a), exhibiting a little lower of phosphorus release, approximately 4 mg/g at pH 1.0, and much lower of phosphorus releases ($<$0.21 mg/g) at the initial pH of 3.0–13.0. The phenomenon is proposed to be due to precipitations between phosphate and metal ions such as calcium, barium and aluminum ions releasing from the BS or PG. The phosphorus release trend of BS-PG1 and BS-PG3 is consistent with the change trends of pH (Fig. 3b). The pH changes can be explained by the large proportion

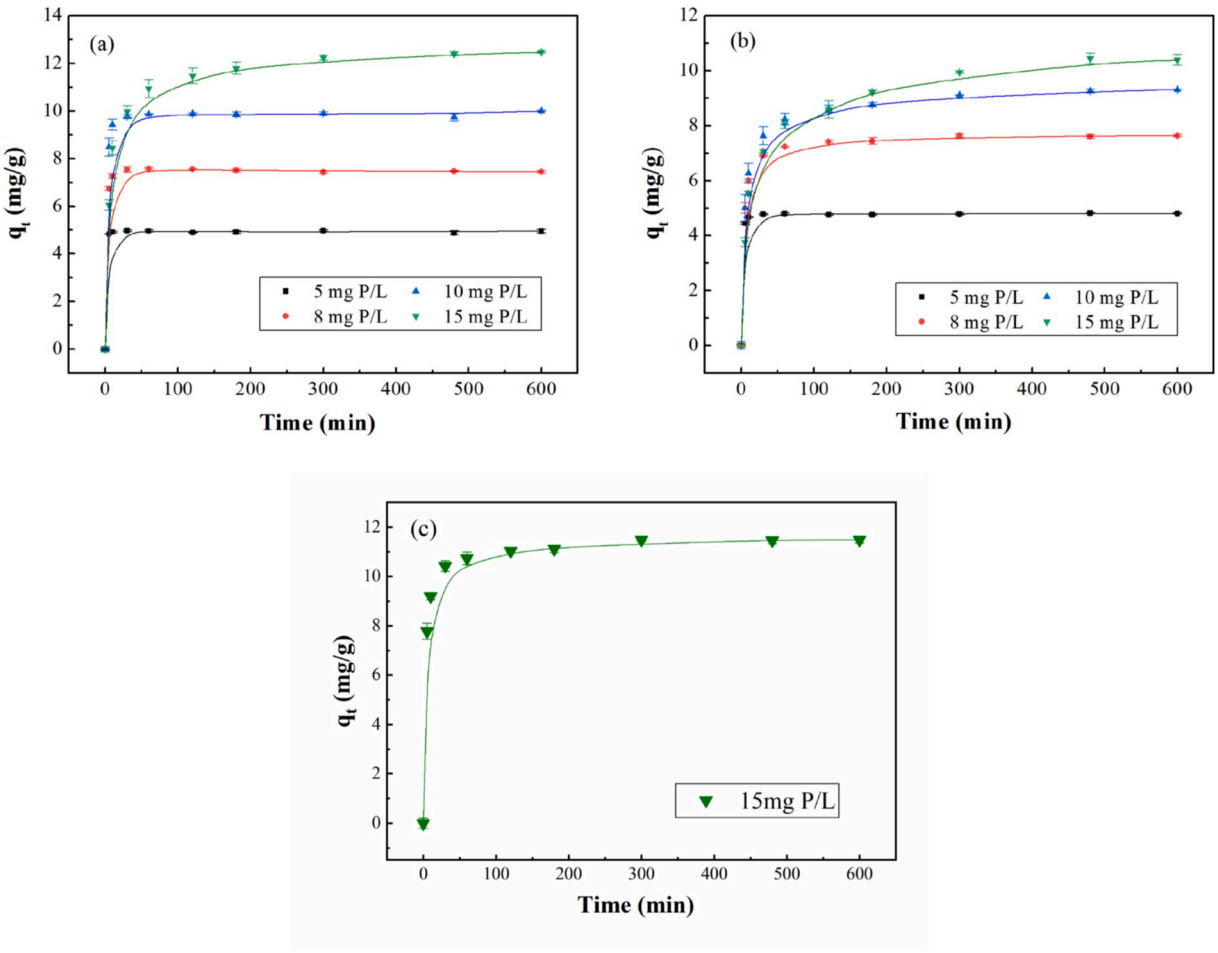

Fig. 4. Effects of contact time on the adsorption of phosphate onto (a) BS-PG1, (b) BS-PG3, and (c) BS.

of BS in which alkaline is dominant.

Although PG releases soluble phosphorus, and BS can release a small amount of phosphorus, BS treated with PG can immobilize the soluble barium and reduce the release of phosphorus. Therefore, BS-PG1 and BS-PG3 can be used as adsorbents for phosphate removal.

3.3. Batch adsorption experiments

3.3.1. Effect of reaction time and phosphorus concentration

Fig. 4 presents the results of kinetic adsorption of phosphate on BS using 15 mg P/L phosphate solutions, and on BS-PG1 and BS-PG3 using 5, 8, 10, and 15 mg P/L phosphate solutions. The condition was controlled at 25 °C, natural pH and with a shaking rate of 200 rpm. The adsorptions to attain equilibrium for BS, BS-PG1, and BS-PG3 with 15 mg P/L as initial concentration are in approximately 3 h. At equilibrium, the adsorption capacity of BS-PG1 and BS-PG3 for phosphate was up to 12.47 and 10.39 mg P/g, respectively (Fig. 4a and b), and their phosphate removal efficiency was calculated as high as 83.21% and 66.18%, respectively. Meanwhile, the equilibrium adsorption capacity of the original BS on the 15 mg/L phosphate solution was as high as 11.49 mg P/g (Fig. 4c). It can be found that the phosphate removal efficiency of each group increased rapidly in the first 60 min. Especially for low-concentration phosphorus solutions, the amount of adsorption in the first 60 min accounts for more than 80% of the total adsorption capacity of equilibrium stage. Phosphate uptake becomes much slower until it reaches equilibrium, which may be due to the decreased diffusion rate (Karaca et al., 2006). The adsorption rate was relatively fast at the beginning as the result of phosphorus ions quickly saturated the exterior surface active sites, and after that the phosphate ions entered into the interior particles (Jellali et al., 2011).

The equilibrium time depends on the initial phosphorus concentrations. The adsorptions to attain equilibrium for BS-PG1 and BS-PG3 with 5, 8, and 10 mg P/L as initial concentrations are in 60 min, while as mentioned with 15 mg P/L are of approximately 3 h. Meanwhile, the equilibrium adsorption capacity also depends on initial adsorbate concentration (Lin et al., 2018). As the curves shown in Fig. 4a and b, the adsorption equilibrium of both BS-PG1 and BS-PG3 increases with the phosphate concentration increasing, because the driving force provided by initial phosphate concentration could overcome the resistance of phosphate mass transfer (Lin et al., 2018). Furthermore, using the initial phosphorus concentration of 5, 8, and 10 mg P/L, BS-PG1 reached respectively 4.95, 7.59, and 9.88 mg P/g, and BS-PG3 was corresponding to 4.81, 7.24, and 8.24 mg P/g. However, with the increasing of initial phosphate concentration in sequence of 5, 8, 10 and 15 mg P/L, the phosphate removal efficiency gradually declines as shown in Table S1. This can be explained by the limited numbers of active sites of the adsorbents for high concentration systems.

As mentioned above, at the initial phosphate concentration of 15 mg P/L, BS-PG1 exhibits a higher adsorption capacity than BS does, while BS-PG3 shows a bit lower adsorption capacity than BS does. Since BS will release harmful ions and presents a relatively low adsorption capacity compared to BS-PG1, its adsorption performance was not further explored for the other phosphate concentration. In addition, BS-PG1 presents a higher adsorption capacity than BS-PG3 in various initial phosphate concentration as shown in Fig. 4a and b, implying a promotion of adsorption when a small amount of PG introduced and a reduction of adsorption when a larger proportion of PG added. This can be attributed to the presence of Ca^{2+} provided by PG, which can precipitate

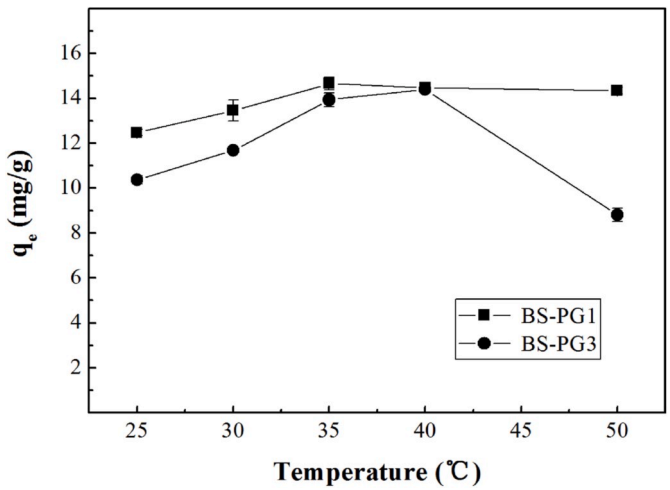

Fig. 5. Effects of solution temperature on the adsorption capacity, using 15 mg P/L of initial concentration under the condition of 0.25g:250 mL and natural pH.

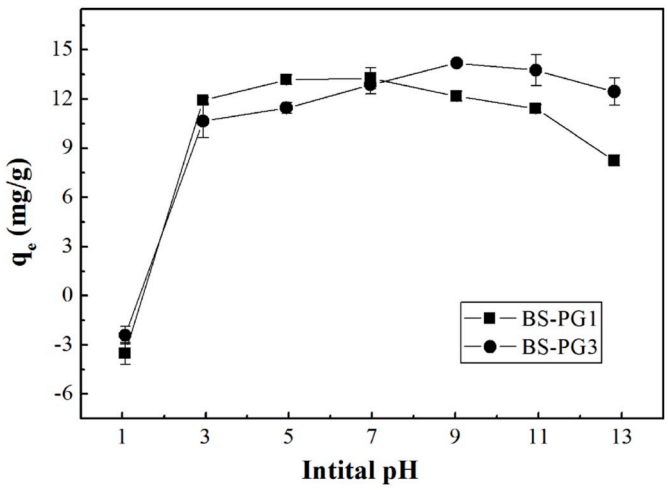

Fig. 6. Effects of solution pH on the adsorption capacity, using 15 mg P/L of initial concentration under the condition of 0.25g:250 mL, 25 °C.

with phosphate (Cusack et al., 2018). On the other hand, adding a high proportion of PG signify less BS inside which makes main contributions to the absorption behavior. Due to this reason, when the proportion of PG is excessive, e.g. a proportion of 10:3 in BS-PG3, it presents decreasing adsorption capacities (Fig. 4b).

3.3.2. *Effect of temperature and initial pH*

The effect of temperature on the phosphate adsorption capacity at 15 mg P/L under the condition of 0.25g:250 mL and natural pH was investigated and the results are shown in Fig. 5. The influence of reaction temperature on the two adsorbents was different. It is apparent that the phosphate adsorption capacity of BS-PG1 increases with the reaction temperature increasing up to 35 °C, and no higher adsorption capacity is obtained when the temperature is higher than 35 °C. As for BS-PG3, a much more distinct increase of phosphate adsorption capacity can be observed when the temperature rises from 25 to 40 °C. The maximum phosphate adsorption capacity reached 14.40 mg P/g at the reaction temperature of 40 °C. However, when the reaction temperature continues to rise to 50 °C, the adsorption phosphate capacity of BS-PG3 drops sharply. These results could be explained by the difference in the amount of PG added. It is reported that the temperature of solution may affect on hydrolysis reactions, precipitation and solubility of the metal hydroxide (Zhao et al., 2011). Metal ions are easier to be soluble at high temperatures, and the release of metal ions in BS-PG1 and BS-PG3 (e.g. Ca^{2+}, Al^{3+}, Fe^{3+}) increases and promotes precipitates with phosphate, resulting in an obvious improve of adsorption capacity. Meanwhile, solution temperature can affect the strength the molecular interactions (Islam et al., 2018). Increasing the temperature enhances the diffusion rate of phosphate and increases the number of surface sites available.

In the process of phosphate removal in this study, adsorption process accompanies with precipitation reaction. The amount of PG added in BS-PG3 is higher than that in BS-PG1 with different final pH levels (Fig. S1), and the precipitation of calcium phosphate accounts for a higher proportion of phosphate removal. When the adsorption process was subjected to high temperature, the calcium phosphate precipitating from the solution dissolved back into the system. This could be assigned to the fact that the removal amount of BS-PG3 declined sharply at 50 °C.

The pH of the solution plays an important role during the adsorption process. In this study, at 25 °C, 250 mL 15 mg P/L solutions containing 0.25 g BS-PG1 or BS-PG3 were adjusted to different pH values ranging from 1.0 to 13.0, to investigate the effect of pH on equilibrium adsorption of phosphate, and the results are illustrated in Fig. 6. There is no removal of phosphate at initial pH of 1.0 with low final pH values as seen in Fig. S2, and the negative data of q_e in Fig. 6 suggest that the equilibrium concentrations are higher than the initial ones, implying a releasing of phosphorus during the process. This results are consistent with the conclusion of the previous blank release (seen in Fig. 3a) . A high adsorption capacity achieves when the pH moves to 3.0, and the adsorption capacity of phosphate increases for both BS-PG1 and BS-PG3 with the increasing of pH. At the pH of 7.0 for BS-PG1 and 9.0 for BS-PG3, they attained their maximum adsorption capacities of 13.27 and 14.20 mg P/g, respectively. This results can be explained by that the higher pH favors the combination of calcium ions and phosphate to form precipitates, which is beneficial to the removal of phosphate (Kamiyango et al., 2009). On the other hand, when the pH rises from 7.0 to 13.0 for BS-PG1, and from 9.0 to 13.0 for BS-PG3, the adsorption rates drop slightly. This is proposed to be due to competition between phosphate and OH^-. The predominant OH^- competes with phosphate ions for adsorption active sites (Xue et al., 2009), and also competes for combination with Ca^{2+} to precipitate, which can also be inferred that BS-PG3 has high soluble calcium ions to consume OH^- to maintain insensitive changes of phosphate adsorption capacity.

3.3.3. *Kinetic studies on phosphate removal*

To further discuss the kinetics of adsorption and the efficiency of BS-PG1 and BS-PG3, the experimental data obtained in this study were employed to derive the kinetic parameters using the two different models: the pseudo-first-order model and pseudo-second-order model (Ye et al., 2015), which can be described below in Eqs. (2) and (3).

$$\text{Pseudo}-\text{first}-\text{order}\ \ \text{equation:}\ \ \ln(q_e - q_t) = \ln q_e - k_1 t \tag{2}$$

$$\text{Pseudo}-\text{second}-\text{order}\ \ \text{equation:}\ \ \frac{t}{q_t} = \frac{1}{k_2 q_e^2} + \frac{t}{q_e} \tag{3}$$

where q_e (mg/g) is the equilibrium adsorption amount of phosphorus, q_t (mg/g) is the adsorption amount of phosphate at time t (min), k_1 and k_2 are the equilibrium rate constant of pseudo-first-order and pseudo-second-order, respectively.

The calculated kinetics parameters are presented in Table 1, in which $q_{e,exp}$ refers to the q_e value obtained from the experiment, while $q_{e,cal}$ is the q_e value calculated from the fitting kinetic equations, and the simulated curves of pseudo-second-order equation shown for BS-PG1 and BS-PG3 are in Fig. 7a and b, respectively. As to the pseudo-first-order model, the values of correlation coefficient (R^2) are relatively lower, and the q_e values between the experiment ($q_{e,exp}$) and calculation ($q_{e,cal}$) possess are considerable different. Therefore, the reaction

Table 1
Pseudo-first-order and pseudo-second-order kinetic model parameters for phosphate removal.

		Pseudo-first-order kinetic equation			Pseudo-second-order kinetic equation		
	$q_{e,exp}$ mg P/g	$q_{e,cal}$ mg P/g	k_1	R^2	$q_{e,cal}$ mg P/g	k_2	R^2
BS-PG1	4.9340	0.0970	0.0884	0.4816	4.9213	0.8358	0.9999
	7.6086	0.9142	0.0718	0.8021	7.4806	0.5623	0.9999
	10.0075	0.3475	0.0022	0.0121	9.9147	0.1397	0.9997
	12.4654	3.6841	0.0088	0.9492	12.5534	0.0117	0.9997
BS-PG3	4.8082	0.1100	0.0077	0.4102	4.8151	0.4852	0.9999
	7.6338	1.1311	0.0092	0.8526	7.6581	0.0456	0.9999
	9.3127	2.5991	0.0084	0.9471	9.3659	0.0165	0.9997
	10.3930	4.4358	0.0084	0.9656	10.0664	0.0081	0.9987

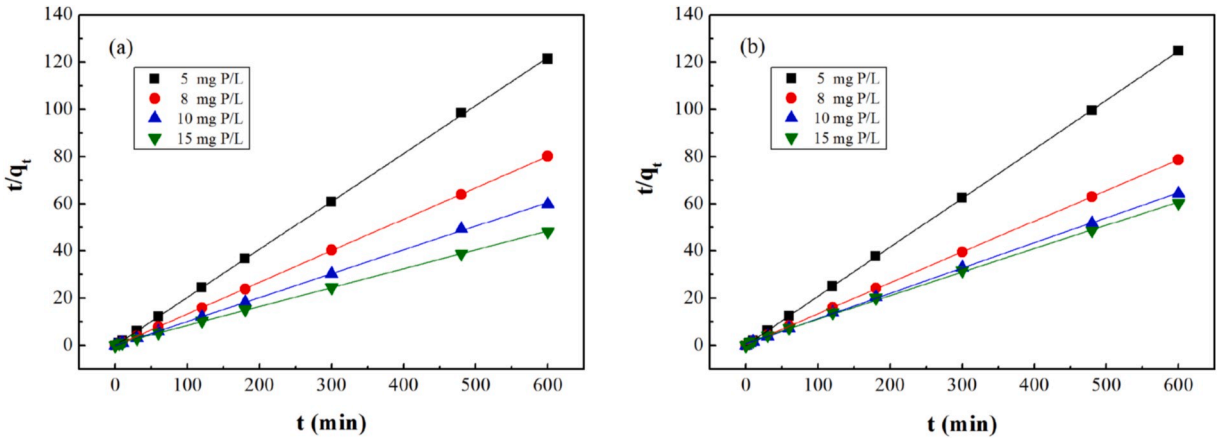

Fig. 7. The simulated pseudo-second-order kinetics of (a) BS-PG1 and (b) BS-PG3.

involved in the system of BS-PG1 and BS-PG3 is not of pseudo-first-order. By contrast, the pseudo-second-order model has higher R^2 (>0.99) and the measured $q_{e,cal}$ is very close to the experimental $q_{e,exp}$. As a result, it can be concluded that the adsorption processes in this study are consistent with the pseudo-second-order kinetic model.

Pseudo-second-order kinetic model generally means that the mechanism of phosphate removal is mainly controlled by chemical bonding or chemisorption (Guo et al., 2018; Jellali et al., 2011). The adsorption process might occur at the active sites on the surface of the BS-PG1 and BS-PG3. Therefore, the adsorption process can be explained as sharing or exchange of electrons at active sites, chemical complexation and precipitation on the adsorbent surface (Bhakat et al., 2006; Jellali et al., 2011).

3.3.4. Adsorption isotherm

It is important to deduce the capacity of the adsorbent using adsorption isotherms. In this study, Langmuir and Freundlich isotherms were applied to describe the adsorption mechanisms, which can be expressed as Eqs. (4) and (5) (Jellali et al., 2011).

$$\text{Langmuir equation: } q_e = q_{max}\frac{K_L C_e}{1 + K_L C_e} \tag{4}$$

$$\text{Freundlich equation: } q_e = K C_e^{1/n} \tag{5}$$

where q_e (mg/g) is equilibrium adsorption amount of phosphorus on adsorbent, q_{max} (mg/g) is the theoretical maximum capacity of the adsorbent, K_L is adsorption constant, and C_e (mg/L) is the concentration of the phosphate solution at equilibrium. In the equation of Freundlich model, K ((mg/g)·(mg/L)$^{-1/n}$) and n (dimensionless) are constant associated with the adsorption capacity of the adsorbent and the intensity of the adsorption (Mezenner and Bensmaili, 2009).

Linearized forms of Langmuir and Freundlich isotherm for the phosphate adsorption are shown in Fig. 8 and Fig. S3, respectively, and

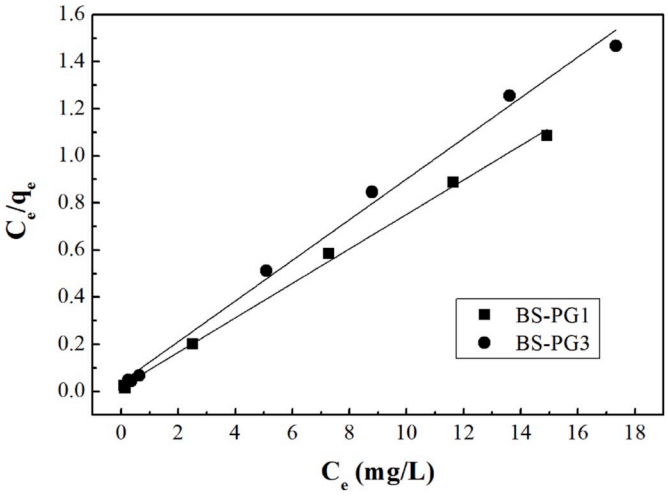

Fig. 8. Linearized form plot of Langmuir isotherm for the adsorption of phosphate onto the adsorbents (adsorbent dosage 0.25 g:250 mL, contact time 10 h, T = 25 °C).

Table 2
Parameters of the Langmuir and Freundlich isotherm for phosphate adsorption.

Sample	Model	Parameters		R^2
BS-PG1	Langmuir	$K_L = 3.764$	$q_{max} = 13.665$	0.9978
	Freundlich	$K = 9.446$	$1/n = 0.1499$	0.6356
BS-PG3	Langmuir	$K_L = 2.229$	$q_{max} = 11.589$	0.9937
	Freundlich	$K = 7.861$	$1/n = 0.142$	0.6649

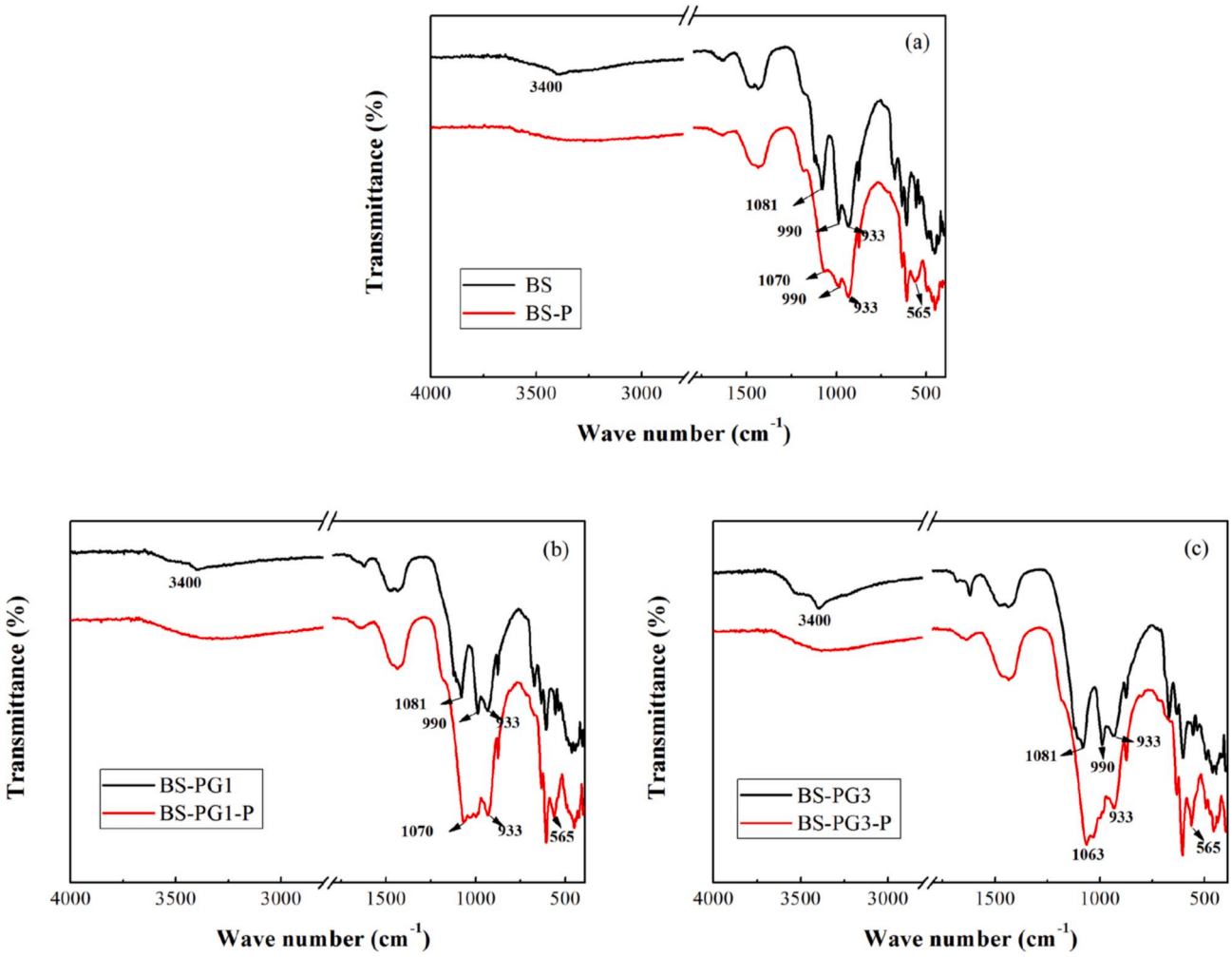

Fig. 9. FTIR spectra of (a) BS, (b) BS-PG1 and (c) BS-PG3 before and after adsorption of phosphate.

the relative isotherm parameters obtained from the intercept and slope of the linearized fitting from Langmuir or Freundlich equation are tabulated in Table 2. It can be observed that Langmuir model provides better fitting results owing to the higher correlation coefficient values ($R^2 > 0.99$), which are considerably higher than the Freundlich isotherm model ($R^2 < 0.70$). As a consequence, this comparison indicates that the adsorption of phosphate onto the BS-PG1 and BS-PG3 conform with the Langmuir isotherm. The results reveal the adsorption process of BS-PG1 and BS-PG3 are homogeneous monolayer adsorption. The maximum capacities q_{max} of BS-PG1 and BS-PG3 are 13.67 and 11.59 mg P/g, respectively (Table 2). The values of q_{max} in this study appear to have a higher phosphate adsorption capacity than most of the other materials (including prepared from various wastes) as listed in Table S2.

3.3.5. *Adsorption mechanisms*

Fig. 9 shows the FTIR spectra of BS, BS-PG1, and BS-PG3 before and after phosphate adsorption. With respect to original samples before adsorption, the intensity of the band at 3400 cm^{-1} is ascribed to stretching vibration of O–H, and the bands at 1081 and 933 cm^{-1} are attributed to S–O stretching vibration (Tu et al., 2019; Seedevi et al., 2017). After adsorption, FTIR spectra display a certain transmission compared with original materials and some changes are registered in the bands located at 3400, 1081, 990, and 565 cm^{-1}. The disappeared peak at 3400 cm^{-1} indicates ligand exchange between –OH and phosphate. It is worth noting that the characteristic band of O–Si–O stretching vibration at 990 cm^{-1} disappears (Navas et al., 2008), and meanwhile a new band appears at about 565 cm^{-1} assigning to P–O stretching vibration (Kaliaraj et al., 2016). All the above changes suggest that phosphate anions have interacted with SO_4^{2-} and covered on SiO_2. Hence, when ligand exchange process occurs, the phosphate adsorption process can be realized according to the following reactions:

$$2 \equiv R\text{–}SO_4^{2-} + H_2PO_4^- \rightarrow (\equiv R)\text{-}HPO_4 + 2SO_4^{2-} + H^+ \ (2.16<pH<7.21) \quad (6)$$

$$\equiv R\text{–}OH + H_2PO_4^- + H^+ \rightarrow (\equiv R)\text{-}H_2PO_4 + H_2O \ (2.16<pH<7.21) \quad (7)$$

$$2\equiv R\text{–}OH + HPO_4^{2-} \rightarrow (\equiv R)_2\text{-}HPO_4 + 2OH^- \ (7.21<pH<12.36) \quad (8)$$

It can be seen that ligand exchange may be one of the major adsorption mechanisms, and the presence of the ≡R–OH and ≡R–SO_4^{2-} functional groups could contribute to the adsorption process.

Since the materials (BS, BS-PG1 and BS-PG3) contains various metals, the solutions after adsorption equilibrium using 0, 10 and 15 mg P/L at 25 °C, natural pH were assessed to verify the adsorption process. The filtered solutions after adsorption equilibrium were determined and the results are in Table 3. It can be seen that the solutions of BS-PG1 and BS-PG3 exhibit obviously lower concentrations of Ba^{2+} than BS, implying that the non-hazardous treatment process is exactly effective and the solutions have no excess metals ions (Gu et al., 2019). Regarding to the same initial P concentration for the sequence of BS, BS-PG1 and BS-PG3, the Ca^{2+} concentration liberating in the solution is going up due to the addition of PG. However, addition of calcium cannot improve the phosphate removal capacity (Drizo et al., 2006). Actually, in this study the solution of BS-PG1 has a medium calcium concentration but it has a highest phosphate removal capacity. Meanwhile, the P concentrations

Table 3
Concentrations of some ions in different phosphate solutions (mg/L).

Adsorbent	Initial P concentration	Ba	Al	Ca	P	Fe
BS	0	69.5	0.17	35.8	<0.5	<0.01
	10	44.2	0.36	14.9	<0.5	<0.01
	15	30.9	0.02	9.60	2.09	<0.01
BS-PG1	0	6.45	0.46	46.7	<0.5	<0.01
	10	8.72	0.16	29.3	<0.5	<0.01
	15	14.4	<0.01	26.4	1.40	<0.01
BS-PG3	0	0.13	0.56	76.2	<0.5	<0.01
	10	0.27	0.12	64.6	<0.5	<0.01
	15	1.09	0.02	61.6	2.45	<0.01

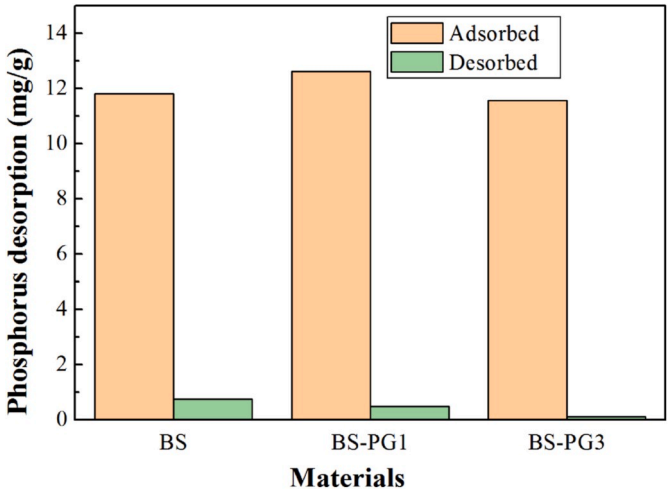

Fig. 10. Adsorption and desorption capacity of phosphate for various materials.

remaining in solution for the three materials at initial concentration of 15 mg P/L as shown Table 3, are consistence with their adsorption capacities as discussed above. Within each group of BS, BS-PG1 and BS-PG3, the concentrations of Ca^{2+} and Al^{3+} decline with the original P concentration increases, implying that the precipitation between phosphate and metal ions exists.

3.4. Desorption experiments

Desorption study was introduced to verify and reveal the adsorption behaviour based on the materials after adsorption using 15 mg P/L as batch adsorption described. Fig. 10 shows the adsorption and desorption capacity of phosphate for BS, BS-PG1, and BS-PG3. As can be seen, all samples show low desorption efficiencies in the aqueous solutions. The desorbability of phosphate for BS, BS-PG1, and BS-PG3 is 6.45, 3.95, and 1.05%, respectively. The results reveal that the phosphate adsorption process is not reversible. In addition, the amount of the desorbed phosphate is slightly decreases with the increasing of PG, which can be attributed to the liberating calcium ions to produce chemical reactions, such as precipitation. Adsorbents of BS-PG1 and BS-PG3 experience mainly a stable and irreversible adsorption process and are suited for removal phosphate application where does not need to recover phosphate or regenerate since they are from industrial waste with low costs.

4. Conclusions

The present work demonstrated that barium slag (BS) treated with phosphogypsum (PG) could be considered as a high effective adsorbent for phosphate removal from aqueous solutions. BS and PG will release phosphorus to the solution when they were individually in the water solutions. BS samples treated with PG (10:1, BS-PG1 and 10:3, BS-PG3) liberate hardly any phosphorus in most pH ranges and can be used as adsorbents for phosphate adsorption. The adsorption capacity for phosphate are 12.47 and 10.39 mg P/g for BS-PG1 and BS-PG3 at the phosphate concentration of 15 mg P/L. In the range of 1.0–13.0, pH affects the removal of phosphate, the optimum pH was found to be 7.0–9.0. As a whole, the adsorption efficiencies of phosphate increase with the increasing of temperature. Pseudo-second-order provides a close agreement with the experimental data for the adsorption kinetics and adsorption isotherm of both BS-PG1 and BS-PG3. The kinetic model studies show that the removal of phosphate is chemisorptions process. Langmuir isothermal adsorption model is in good agreement with experimental data. The findings from the current study indicate that BS-PG1 and BS-PG3 could be used to treat phosphate-containing water.

Author statement

Tengfei Guo: Investigation, Resources, Data Curation, Writing - Original Draft, Hannian Gu: Writing - Review & Editing, Supervision, Funding acquisition, Shicheng Ma: Investigation, Resources, Ning Wang: Supervision.

Declaration of competing interest

The authors declare that they have no known competing financial interests or personal relationships that could have appeared to influence the work reported in this paper.

Acknowledgments

The work was financially supported by National Natural Science Foundation of China (Grant No. U1812402; 41972048).

Appendix A. Supplementary data

Supplementary data to this article can be found online at https://doi.org/10.1016/j.jenvman.2020.110823.

References

Bhakat, P.B., Gupta, A.K., Ayoob, S., Kundu, S., 2006. Investigations on arsenic (V) removal by modified calcined bauxite. Colloid Surface A 281, 237–245.
Cuadri, A.A., Navarro, F.J., García-Morales, M., Bolívar, J.P., 2014. Valorization of phosphogypsum waste as asphaltic bitumen modifier. J. Hazard. Mater. 279, 11–16.
Cusack, P.B., Healy, M.G., Ryan, P.C., Burke, I.T., O'Donoghue, L.M.T., Ujaczki, E., Courtney, R., 2018. Enhancement of bauxite residue as a low-cost adsorbent for phosphorus in aqueous solution, using seawater and gypsum treatments. J. Clean. Prod. 179, 217–224.
Ding, J., 2005. Using barium slag processing wastewater containing chromium (VI). Environ. Prot. Chem. Ind. 25, 225–227 (In Chinese).
Dong, C., Chen, Y., Wang, Y., 2003. Comprehensive utilization of barium containing waste residue. Hebei Chem. Eng. Ind. 5, 53–54 (In Chinese).
Drizo, A., Forget, C., Chapuis, R.P., Comeau, Y, 2006. Phosphorus removal by electric arc furnace steel slag and serpentinite. Water Res. 40, 1547–1554.
Gu, H., Guo, T., Dai, Y., Wang, N., 2019. Non-hazardous treatment for barium slag using phosphogypsum. Waste Biomass Valori. 10, 3157–3161.
Guo, T., Yang, H., Liu, Q., Gu, H., Wang, N., Yu, W., Dai, Y., 2018. Adsorptive removal of phosphate from aqueous solutions using different types of red mud. Water Sci. Technol. 2017 (2), 570–577.
Guzmán, D., Fernández, J., Ordoñez, S., Aguilar, C., Rojas, P.A., Serafni, D., 2012. Effect of mechanical activation on the barite carbothermic reduction. Int. J. Miner. Process 102–103, 124–129.
Islam, Md.A., Morton, D.W., Johnson, B.B., Pramanik, B.K., Mainali, B., Angove, M.J., 2018. Metal ion and contaminant sorption onto aluminium oxide-based materials: a review and future research. J. Environ. Chem. Eng. 6, 6853–6869.
Jamshidi, E., Ebrahim, H.A., 2008. A new clean process for barium carbonate preparation by barite reduction with methane. Chem. Eng. Process 47, 1567–1577.
Jellali, S., Wahab, M.A., Hassine, R.B., Hamzaoui, A.H., Bousselmi, L., 2011. Adsorption characteristics of phosphorus from aqueous solutions onto phosphate mine wastes. Chem. Eng. J. 169, 157–165.
Jiang, G., Wu, A., Wang, Y., Li, J., 2019. The rheological behavior of paste prepared from hemihydrate phosphogypsum and tailing. Constr. Build. Mater. 229, 116870.
Jiang, R., 2007. Study of barium slag gelling and activating property and application. Coal Ash China 19, 24–26 (In Chinese).

Kaliaraj, G.S., Kirubaharan, K., Pradhaban, G., Kuppusami, P., Vishwakarma, V., 2016. Isolation and characterization of biogenic calcium carbonate/phosphate from oral bacteria and their adhesion studies on YSZ-coated titanium substrate for dental implant application. B. Mater Sci. 39, 385–389.
Kamiyango, M.W., Masamba, W.R.L., Sajidu, S.M.I., Fabiano, E., 2009. Phosphate removal from aqueous solutions using kaolinite obtained from Linthipe, Malawi. Phys. Chem. Earth 34 (13–16), 850–856.
Karaca, S., Gurses, A., Ejder, M., Acikyildiz, M., 2006. Adsorptive removal of phosphate from aqueous solutions using raw and calcinated dolomite. J. Hazard. Mater. 128, 273–279.
Lamb, D.T., Matanitobua, V.P., Palanisami, T., Megharaj, M., Naidu, R., 2013. Bioavailability of barium to plants and invertebrates in soils contaminated by barite. Environ. Sci. Technol. 47, 4670–4676.
Li, F., Liu, J., Yang, G., Pan, Z., Ni, X., Xu, H., Huang, Q., 2013. Effect of pH and succinic acid on the morphology of α-calcium sulfate hemihydrate synthesized by a salt solution method. J. Cryst. Growth 374, 31–36.
Li, X., Du, J., Gao, L., He, S., Gan, L., Sun, C., Shi, Y., 2017. Immobilization of phosphogypsum for cemented paste backfill and its environmental effect. J. Clean. Prod. 156, 137–146.
Lin, J., Jiang, B., Zhan, Y., 2018. Effect of pre-treatment of bentonite with sodium and calcium ions on phosphate adsorption onto zirconium-modified bentonite. J. Environ. Manag. 217, 183–195.
Liu, L., Jia, S., Wang, Y., Chen, Y., Zhang, Q., Yang, L., 2017. Study on application of barium residue in building materials and effect of heavy metal curing. Brick-Tile 5, 25–27 (In Chinese).
Liu, Q., Chen, W., Zhang, X., Yu, L., Zhou, J., Xu, Y., Qian, G., 2015. Phosphate enhancing fermentative hydrogen production from substrate with municipal solid waste composting leachate as a nutrient. Bioresour. Technol. 190, 431–437.
Liu, X., Zhao, J., Yan, J., Jiang, Y., Liu, Z., Yu, T., 2016. The invention relates to a harmless treatment method for barium slag. Chinese Patent. CN 106734056 A. (In Chinese).
Lopes, G., Guilherme, L.R.G., Costa, E.T.S., Curi, N., Penha, H.G.V., 2013. Increasing arsenic sorption on red mud by phosphogypsum addition. J. Hazard. Mater. 262, 1196–1203.
Menzie, C.A., Southworth, B., Stephenson, G., Feisthauer, N., 2008. The importance of understanding the chemical form of a metal in the environment: the case of barium sulfate (barite). Hum. Ecol. Risk Assess. 14, 974–991.
Mezenner, N.Y., Bensmaili, A., 2009. Kinetics and thermodynamic study of phosphate adsorption on iron hydroxide-eggshell waste. Chem. Eng. J. 147 (2–3), 87–96.
Mulopo, J., Motaung, S., 2014. Carbothermal reduction of barium sulfate-rich sludge from acid mine drainage treatment. Mine Water Environ. 33, 48–53.
Navas, N., Romero-Pastor, J., Manzano, E., Cardell, C., 2008. Benefits of applying combined diffuse reflectance FTIR spectroscopy and principal component analysis for the study of blue tempera historical painting. Anal. Chim. Acta 630, 141–149.
Papaslioti, E.-M., Pérez-López, R., Parviainen, A., Sarmiento, A.M., Nieto, J.M., Marchesi, C., Delgado-Huertas, A., Garrido, C.J., 2018. Effects of seawater mixing on the mobility of trace elements in acid phosphogypsum leachates. Mar. Pollut. Bull. 127, 695–703.
Rashad, A.M., 2017. Phosphogypsum as a construction material. J. Clean. Prod. 166, 732–743.
Sakai, S., Anada, T., Tsuchiya, K., Yamazaki, H., Margolis, H.C., Suzuki, O., 2016. Comparative study on the resorbability and dissolution behavior of octacalcium phosphate, β-tricalcium phosphate, and hydroxyapatite under physiological conditions. Dent. Mater. J. 35, 216–224.
Salem, A., Jamshidi, S., 2012. Effect of paste humidity on kinetics of carbothermal reduction of extruded barite and coke mixture. Solid State Sci. 14, 1012–1017.
Salem, A., Osgouei, Y.T., 2009. The effect of particle size distribution on barite reduction. Mater. Res. Bull. 44, 1489–1493.
Seedevi, P., Moovendhan, M., Viramani, S., 2017. Bioactive potential and structural chracterization of sulfated polysaccharide from seaweed (Gracilaria corticata). Carbohyd. Polym. 155, 516–524.
State Environmental Protection Administration SEPA, 2007. General administration of quality supervision, inspection and quarantine (AQSIQ). Identification Standards for Hazardous Wastes: Identification for Extraction Toxicity. The National Standard of the P. R. China. GB 5085.3-2007.
Tu, C.H., Hsu, S.L.C., Bulycheva, E., Belomoina, N., 2019. Novel crosslinked AB-type polyphenylquinoxaline membranes for high-temperature proton exchange membrane fuel cells. Polym. Eng. Sci. 59, 2169–2173.
Vaidya, R., Kodam, K., Ghole, V., Surya, M.R.K., 2010. Validation of an in situ solidification/stabilization technique for hazardous barium and cyanide waste for safe disposal into a secured landfill. J. Environ. Manag. 91, 1821–1830.
Wang, X., Yan, X., Li, X., 2016. Research on pollution characteristics and resource utilization risk of barium slag. J. Environ. Technol. 6, 170–174 (In Chinese).
Xue, S., Li, M., Jiang, J., Millar, G.J., Li, C., Kong, X., 2019. Phosphogypsum stabilization of bauxite residue: conversion of its alkaline characteristics. J. Environ. Sci. 77, 1–10.
Xue, Y., Hou, H., Zhu, S., 2009. Characteristics and mechanisms of phosphate adsorption onto basic oxygen furnace slag. J. Hazard. Mater. 162, 973–980.
Yao, J., Zhao, Y., 2010. Phosphorus removal from wastewater by synergistic effect of barium residue and lime. Environ. Sci. Technol. 33, 163–173 (In Chinese).
Ye, J., Cong, X., Zhang, P., Erhard, H., Zeng, G., Wu, Y., Zhang, H., Fan, W., 2015. Phosphate adsorption onto granular-acid-activated-neutralized red mud: parameter optimization, kinetics, isotherms, and mechanism analysis. Water Air Soil Poll. 226, 306.
Yuan, Z., Li, Z., Xia, J., 2016. Research on pretreatment condition of barium residue before admission. J. Wuhan Univ. Technol. 38, 67–71 (In Chinese).
Zhao, Y., Zhang, L., Ni, F., Xi, B., Xia, X., Peng, X., Luan, Z., 2011. Evaluation of a novel composite inorganic coagulant prepared by red mud for phosphate removal. Desalination 273, 414–420.